JOURNAL OF MATERIALS SCIENCE 10 (1975) 1093–1104

An X-ray Fourier line shape analysis in cold-worked hexagonal metals

Part 2 *Titanium, magnesium and zinc*

S. K. CHATTERJEE, S. P. SEN GUPTA
Department of General Physics and X-rays, Indian Association for the Cultivation of Science, Calcutta 700032, India

Detailed Fourier analysis of line shapes using the technique of Warren, has been performed on cold-worked hexagonal magnesium, zinc and titanium and a partially recovered state of titanium at room temperature. X-ray diffraction profiles from fault-unaffected 10.0, 00.2, 11.0, 20.0, 11.2, 00.4 and fault-affected 10.1, 10.2, 10.3, 20.1 and 20.2 reflections have been recorded in a Geiger counter diffractometer with copper radiation and the microstructural parameters have been evaluated. A small anisotropy in both domain sizes and root mean square strains has been observed for these materials; this is similar to the study on zirconium in Part 1. The average values of these are, respectively, of the order of 380 Å and 1.58×10^{-3} for titanium in the cold-worked state with a small recovery on annealing, 1650 Å and 0.71×10^{-3} for magnesium, and 1060 Å and 0.57×10^{-3} for zinc. Least-squares analysis applied to fault-affected reflections has yielded very small concentrations of deformation faults, α ($\simeq 8.0 \times 10^{-3}$), and growth faults, β ($\simeq 2.0 \times 10^{-3}$), in the cold-worked state of titanium similar to those in zirconium, and negligible concentrations of these ($\alpha \simeq 0.63 \times 10^{-3}$, $\beta \simeq 0.21 \times 10^{-3}$) in magnesium. The presence of deformation and growth faults could not be detected in zinc, possibly due to considerable recovery. An estimate of stacking-fault energy, γ, has also been made in titanium and magnesium from an expression taking basal slip and the value of α into account, and this has been found to be quite low for both materials. The favourable slip mode in these hexagonal metals has been discussed in the light of the experimental results.

1. Introduction

A detailed Fourier analysis of line shapes [1] has recently been carried out in hexagonal zirconium for both the cold-worked and partially recovered states in Part 1 by Chatterjee and Sen Gupta [2]. Quantitative information on the coherent domain sizes, microstrains within these domains, and the occurrence of deformation and growth stacking faults in zirconium has been obtained from this analysis bearing in mind the maximum number of observable X-ray diffraction profiles. The analysis has shown a small anisotropy in the domain sizes and strains, and a very small concentration of deformation stacking faults; growth faults do not appear to exist. The present investigation is concerned with three other important hexagonal metals, i.e. titanium, magnesium and zinc, and forms Part 2 of our present programme of systematically studying the hexagonal metals by X-ray diffraction methods taking into account the maximum number of observable reflections in the cold-worked state. The importance of this study has been emphasized in Part 1.

The metals titanium and zirconium belong to group IVB of the periodic table and crystallize in the same two allotropic modifications in the solid state, both having approximately the same c/a axial ratio (~ 1.59) for the hexagonal phases. Contrary to this, both magnesium and zinc belong to group II of the periodic table and have a relatively low melting point ($\sim$ 650 and $\sim 419.5°C$ respectively) with a slightly different ratio for close-packing ($c/a \sim 1.62$ for Mg and ~ 1.85 for Zn). Previous X-ray studies on titanium [3-5] and magnesium [4, 6-7] considered fewer diffraction profiles and hence were inconclusive in obtaining a fairly representative

picture of the microstructure which develops in the deformed state of these materials. In our present measurements, the line-shape analysis for the fault-unaffected (10.0, 00.2, 11.0, 20.0, 11.2 and 00.4) and with fault-affected, (10.1, 10.3, 20.1, 10.2 and 20.2) reflections have been considered in detail for the cold-worked states of titanium, magnesium and zinc at room temperature (25 ± 1°C) and also for the partially recovered state of titanium (annealed at 550°C for 16 h).

2. Experimental procedure

The procedure used has already been described in detail in Part 1, but is briefly summarized below.

The cold-worked samples were prepared by hand-filing spectroscopically pure titanium, magnesium and zinc (Johnson Matthey Chemicals Ltd, London). Flat diffractometer samples representing the cold-worked state at room temperature (25 ± 1°C), the partially recovered state and fully annealed state (for titanium 800°C for 12 h and much less near the recrystallization temperature for magnesium and zinc) were prepared as given in Part 1. The chart recording followed by fixed-time point counting at intervals of 0.1 to 0.01° in 2θ was done using a Philips counter diffractometer (PW 1050, 51) employing nickel-filtered Cu$K\alpha$ radiation. The line profiles from the annealed specimens have been considered as "standards" for the instrumental broadening correction by Stokes' method [8].

2.1. Fourier line-shape analysis

The line-shape analysis as outlined by Warren [1] is restricted to basal slip, i.e. slip on the 00.2 plane of the hcp structure. Stokes' corrected Fourier coefficients, A_L, were obtained using a program written for IBM 1130 and these are utilized in evaluating the parameters D, $\langle\epsilon^2\rangle$, α and β, from the following equations, as given in Part 1. The symbols have their usual meanings [1, 2].

$$A_L = A_L{}^{\mathrm{S}} \,.\, A_L{}^{\mathrm{D}} \tag{1}$$

where

$$A_L{}^{\mathrm{D}} = \exp(-2\pi^2 L^2 \langle \epsilon_L{}^2 \rangle / d^2) \tag{2}$$

and

$$-\left(\frac{\mathrm{d}A_L{}^{\mathrm{S}}}{\mathrm{d}L}\right)_0 = \frac{1}{D}, \text{ for } H\text{-}K = 3N \tag{3.1}$$

$$-\left(\frac{\mathrm{d}A_L{}^{\mathrm{S}}}{\mathrm{d}L}\right)_0 = \frac{1}{D_{\mathrm{e}}} = \frac{1}{D} + \frac{|L_0|d}{c^2}(3\alpha + 3\beta)$$
$$\text{for } H\text{-}K = 3N \pm 1, L_0 \text{ even} \tag{3.2}$$

$$-\left(\frac{\mathrm{d}A_L{}^{\mathrm{S}}}{\mathrm{d}L}\right)_0 = \frac{1}{D_{\mathrm{e}}} = \frac{1}{D} + \frac{|L_0|d}{c^2}(3\alpha + 3\beta)$$
$$\text{for } H\text{-}K = 3N \pm 1, L_0 \text{ odd}. \tag{3.3}$$

2.2. Dislocation density and stacking fault energy

The dislocation density, ρ, in the materials has been obtained from the relations [9] used in Part 1, considering the absence of extensive polygonization or dislocation pile-ups (i.e. $n \simeq F$):

$$\rho = (\rho_{\mathrm{D}} \,.\, \rho_{\mathrm{S}})^{\frac{1}{2}} \tag{4}$$

where

$$\rho_{\mathrm{D}} \text{ (due to domain size)} = 3/D^2 \tag{5}$$

$$\rho_{\mathrm{S}} \text{ (due to strain } \epsilon) = K\langle\epsilon^2\rangle/\boldsymbol{b}^2 \,. \tag{6}$$

where $\boldsymbol{b}$ is Burger's vector for basal slip, and K is a constant which, in the case of Gaussian strain distribution is 19.5, 19.0 and 18.5 for titanium, magnesium and zinc, respectively.

In hexagonal crystals, the common slip system is on the basal plane in a close-packed direction $(0001)\ \langle 11\bar{2}0\rangle$ and the unit slip vector, $\boldsymbol{b} = \frac{1}{3}[11\bar{2}0]$, dissociates into two partials, $\boldsymbol{b}_1$ and $\boldsymbol{b}_2$, bounding a narrow ribbon of stacking fault. If the equilibrium separation between these two partials is denoted by r, then the deformation fault probability, α, can be defined as

$$\alpha = \rho \,.\, r \,.\, d \tag{7}$$

where ρ is the dislocation density and d the interplanar spacing of the slip plane [10, 11]. At the equilibrium separation of the two partials, the force F repelling them is equal to the energy γ per unit area of the stacking fault (erg cm^{-2} depending on units of F) [12, 13], and is given by

$$\mu(\boldsymbol{b}_1 \,.\, \boldsymbol{b}_2)/2\pi r = F = \gamma \tag{8}$$

where μ is the shear modulus. The strengths of $|\boldsymbol{b}_1|$ and $|\boldsymbol{b}_2|$ are $a/\sqrt{3}$, and the angle between them is found to be 120° [12]. Thus, from Equations 7 and 8 we obtain:

$$\gamma = \mu a^2/(12\pi r) \tag{9}$$

and

$$\alpha = \mu a^2 \,.\, \rho d/(12\pi\gamma) \,. \tag{10}$$

From Equation 10, we obtain an expression for the stacking fault energy:

$$\gamma(\text{erg cm}^{-2}) = \mu a^2 \cdot \rho \cdot d_{00.2}(12\pi\alpha) \quad (11)$$

where the (00.2) plane is considered to be the slip plane.

3. Results and discussion

The normalized Fourier coefficients A_L, after Stokes' correction [8] for the instrumental broadening, are plotted against L (Å) for the cold-worked states of titanium (Figs. 1 and 2), magnesium (Figs. 3 and 4) and zinc (Figs. 5 and 6) considering $H\text{-}K = 3N$ and $H\text{-}K = 3N \pm 1$ (L_0 odd or even) reflections. A small recovery has been observed for titanium (annealed at 550°C for 16 h) from the slight upward trend in the respective A_L coefficients [2]. In Figs. 4 and 6, considerable scattering of the experimental A_L values has been observed for the fault-affected 10.3, 20.1 and 20.2 reflections of magnesium and zinc, due to overlapping and background effects. For fault-unaffected reflections this has only been observed for 00.4 (Figs. 3 and 5). The scattering of experimental points, for magnesium and zinc in particular, has been eliminated by a least-squares fit of a polynomial of the form $A(L) = A_0 + A_1L + A_2L^2$, as shown in Figs. 3 to 6. It may be seen that in most of the cases, the least-squares fitted points lie close to the experimental points and also to the average curves drawn through these.

Fig. 7 shows the log plots for the six fault-unaffected reflections, i.e. 10.0, 00.2, 11.0, 20.0 and 00.4 for a distance L up to 200 Å in the case of titanium. The proximity of the points in this plot reflects considerable isotropy in the domain sizes and strains. This has also been observed in magnesium and zinc (Fig. 8). In the latter case, where the scattering is relatively prominent, least-squares plots have been shown in order to see the consistency of averaging the experimental points for a linear relationship. Similar observations on the small anisotropy were observed earlier for zirconium [2] and also for titanium by Gupta *et al.* [5] who considered only three reflections. For the cold-worked and partially recovered states of titanium, the values of the average domain sizes, D, from the distortion-corrected Fourier coefficients, A_L^S, for these reflections are 380 and 486 Å and the r.m.s. strain values $\langle \epsilon_L^2 \rangle^{\frac{1}{2}}$ at an average distance of $L = 100$ Å are 1.58×10^{-3} and 0.34×10^{-3} respectively (Table I). These values are of similar magnitudes to those observed for zirconium in Part 1 and show small recovery effects in the fragmentation of domains and the consequent removal of strains from these

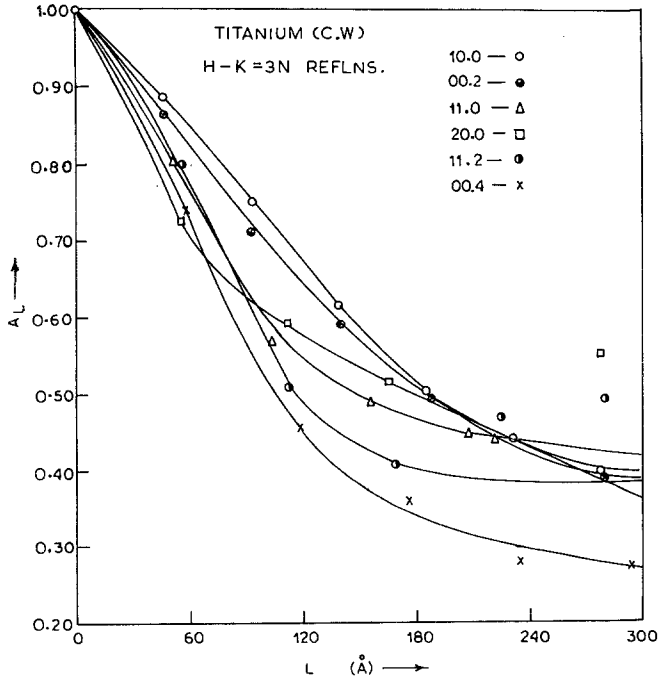

Figure 1 The plot of Fourier coefficients A_L versus L for $H\text{-}K = 3N$ reflections for cold-worked titanium.

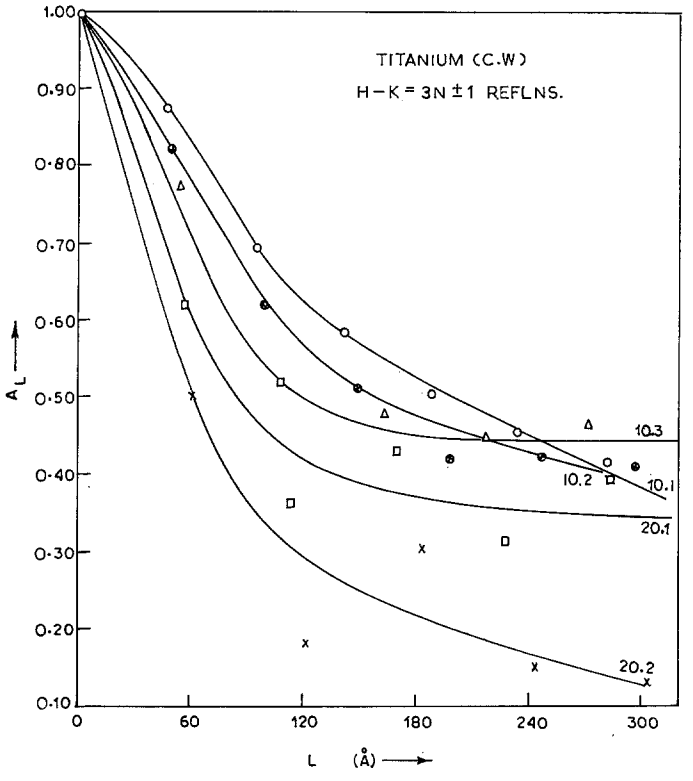

Figure 2 The plot of Fourier coefficients A_L versus L for $H\text{-}K = 3N \pm 1$ reflections for cold-worked titanium.

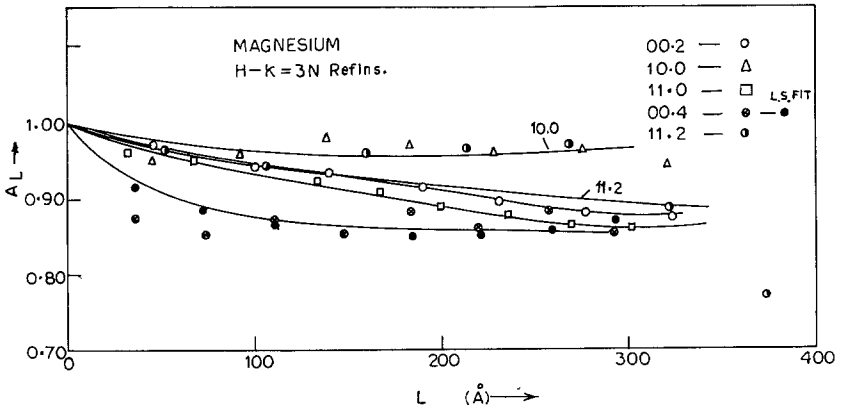

Figure 3 The plots of Fourier coefficients A_L versus L for $H\text{-}K = 3N$ reflections for cold-worked magnesium.

domains. The domain size values are also very close to 380 and 403 Å as reported earlier [4, 5] for cold-worked titanium, determined by considering fewer reflections. The variation of r.m.s. strains $\langle \epsilon_L^2 \rangle^{\frac{1}{2}}$ over the column length, L (Fig. 9), for the cold-worked and the partially recovered states of titanium is in agreement with the usual picture of the dislocation structure that develops in heavily deformed metals and alloys [2]. In the cases of magnesium and zinc, A_L^S versus L plots are shown in Fig. 10 and the values of the domain sizes are 1650 Å for magnesium and 1060 Å for zinc (Table I). These values are much larger than those obtained for zirconium in Part 1 and for titanium. In the case of zinc, A_L^S values obtained from the intercepts of least-squares plots (Fig. 8) are found to lie on the initial portion of the curve drawn from averaging the experimental points, and deviate at higher L (Fig. 10). The r.m.s. strain values $\langle \epsilon_L^2 \rangle^{\frac{1}{2}}$ at

TABLE I Particle size, D, r.m.s. strain $\langle \epsilon_L^2 \rangle^{\frac{1}{2}}$ and dislocation density, ρ, for titanium, magnesium and zinc from fault-unaffected (H-$K = 3N$) reflections

Sample	D (Å)	r.m.s. strain $\langle \epsilon_L^2 = 100 \text{ Å} \rangle^{\frac{1}{2}} \times 10^3$	Dislocation density $\rho \times 10^{-11}$ (cm cm^{-3})
Ti (cold-worked)	380	1.58	1.08
Ti (annealed at 550°C for 16 h)	486	0.34	0.18
Mg	1650	0.71	0.10
Zn	1060	0.57	0.14

TABLE II Effective domain size D_e and fault probability, α and β, for titanium, magnesium and zinc from fault affected (H-$K = 3N \pm 1$) reflections

Sample	Reflections H-$K = 3N \pm 1$	D_e (Å)	Compound fault probability		α and β from L.S. solution		$\alpha \times 10^3$ assuming $\beta = 0$	Mean $\alpha \times 10^3$
			$(3\alpha + \beta)$	$(3\alpha + 3\beta)$	$\alpha \times 10^3$	$\beta \times 10^3$		
Ti (cold-worked)	L_0 odd							
	10.1	302	7.30				2.43	9.38
	10.3	264	6.71				2.24	
	20.1	160	65.47		8.13	2.07	21.82	
	L_0 even							
	10.2	300		4.89			1.63	
	20.2	120		56.41			18.80	
Ti (annealed at 550°C for 16 h)	L_0 odd							
	10.1	500	−0.56				−0.18	1.81
	10.3	260	9.83				3.27	
	20.1	460	2.06		0.58	2.05	0.69	
	L_0 even							
	10.2	314		7.16			2.39	
	20.2	340		8.64			2.88	
Mg	L_0 odd							
	10.1	880	5.80				1.90	0.74
	10.3	1600	0.12				0.04	
	20.1	1600	0.38		0.63	0.21	0.13	
	L_0 even							
	10.2	2000		−0.75			−0.25	
	20.2	880		5.80			1.90	
Zn	L_0 odd							
	10.1	1280						
	10.3	1320						
	20.1	2200						
	L_0 even							
	10.2	1620						
	20.2	1740						

$L = 100$ Å are of the order of 0.71×10^{-3} for magnesium and 0.57×10^{-3} for zinc (Table I). For zinc, this value is 0.62×10^{-3} calculated from the least-squares plots (Fig. 8). In the case of magnesium, the mean values of the domain sizes and r.m.s. strains reported by Lele and Anantharaman [4] from the integral breadth analysis are of the order of 1350 Å and 0.72×10^{-3} respectively, and these values agree well with our present values from Fourier analysis considering that they are obtained by two different methods. The comparatively high particle size and small strain values for both magnesium and zinc in the cold-worked state thus indicate that these effects are quite small in the X-ray line broadening and that the room temperature recovery is quite appreciable in these materials.

For the fault-affected reflections, i.e. 10.1,

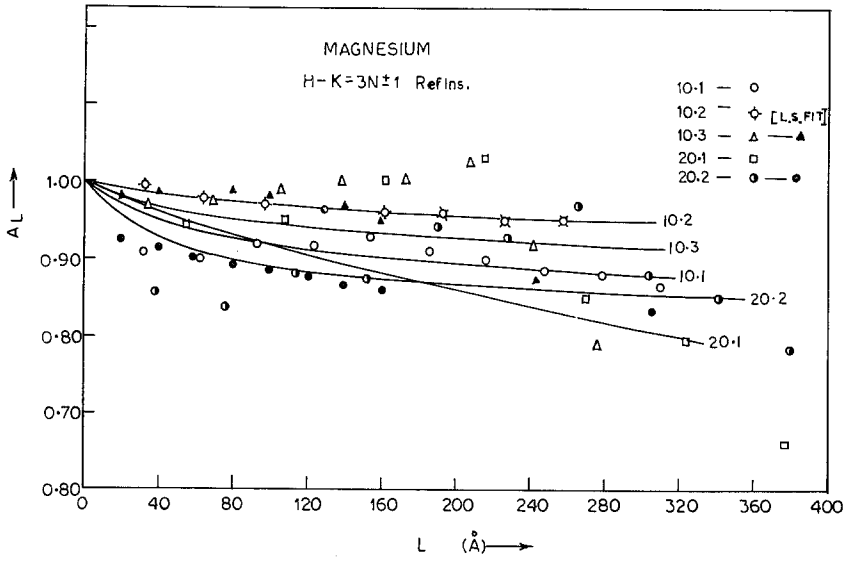

Figure 4 The plot of Fourier coefficients A_L versus L for $H\text{-}K = 3N \pm 1$ reflections for cold worked magnesium.

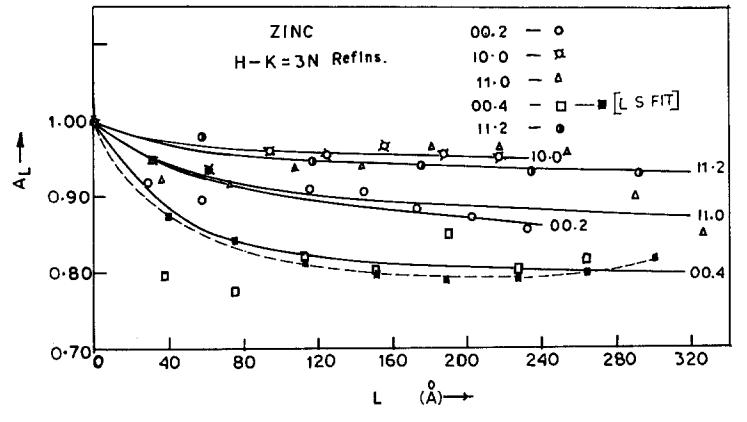

Figure 5 The plot of Fourier coefficients A_L versus L for $H\text{-}K=3N$ reflections for cold-worked zinc.

10.2, 10.3, 20.1 and 20.2, the distortion corrected size coefficients, A_L^S are plotted against L (Å) and shown in Fig. 10 for magnesium and zinc together with the observations from the least squares analysis. The values of the effective particle sizes D_e, determined from the initial straight line region of these plots (Table II, Equations 3.2 and 3.3), are quite close to the average domain size value, D (Table I, Equation 3.1), in all three cases. The values have been found to be slightly less for the 20.1 and 20.2 reflections of titanium and 10.1 and 20.2 reflections of magnesium, indicating that the (10.1) planes are affected by faulting. Similar effects have also been observed earlier for zirconium [2]. However, the closeness between the values of D_e and D suggests small concentrations of stacking faults in the cold-worked state of these materials exist. This has been clearly indicated by a least-squares analysis of the values of the compound fault probabilities $(3\alpha + \beta)$ and $(3\alpha + 3\beta)$ for the corresponding reflections (Table II) using the isotropic domain size value, D, in Equations 3.2 and 3.3. In the case of titanium, this analysis has yielded a value for the deformation fault probability, α, of 8.13×10^{-3} in the cold-worked state, which is of the same order of magnitude as that of zirconium [2] ($\sim 4 \times 10^{-3}$). This is also in close agreement with the value of 8.0×10^{-3} obtained by Lele and Anantharaman [4] from the line-shape analysis of 10.1 and 10.2 reflections but differs

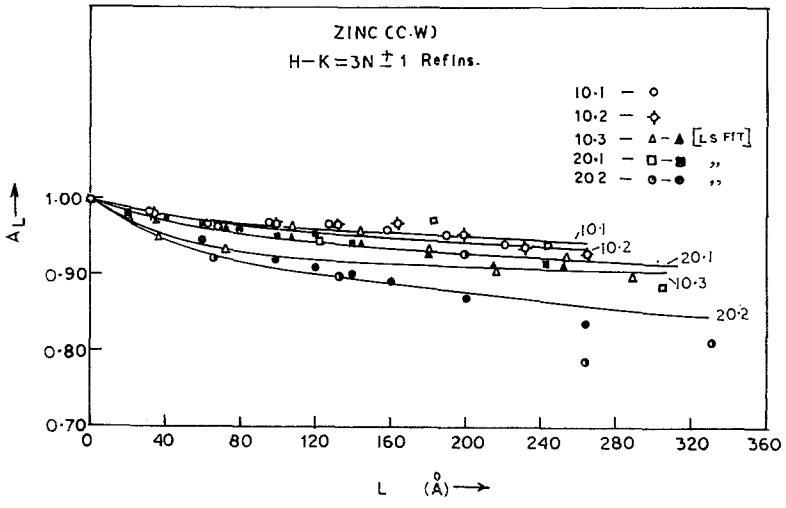

Figure 6 The plot of Fourier coefficients A_L versus L for $H\text{-}K = 3N \pm 1$ reflections for cold-worked zinc.

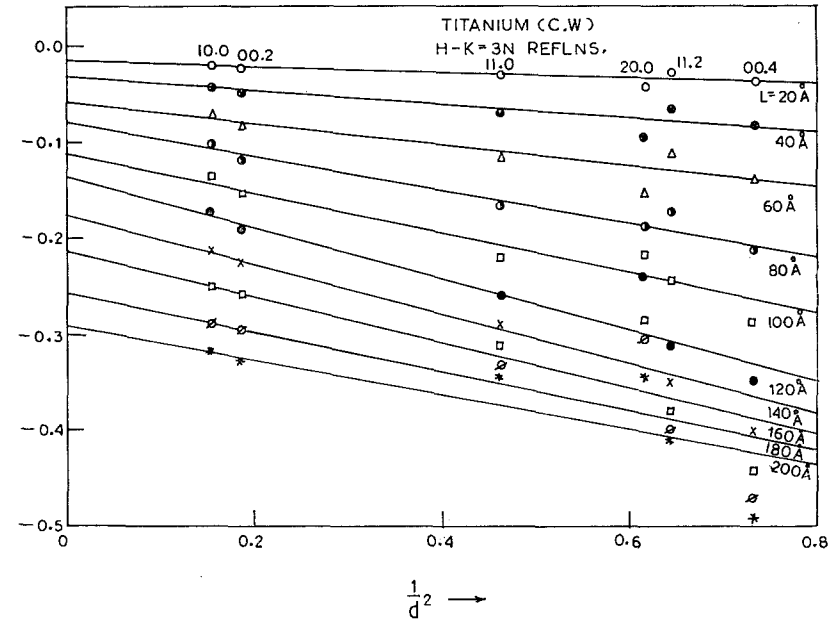

Figure 7 The plot of $\log_{10} A_L$ versus $1/d^2$ for values of L for cold-worked titanium.

considerably from those of Spreadborough and Christian [3] and Gupta *et al.* [5]. The discrepancy is quite possible since in the analysis of Spreadborough and Christian [3] only two high-angle reflections, namely 11.4 and 12.1 ($\theta \simeq 57°$), were considered and Gupta *et al.* [5] have determined $\alpha(\sim 0.1 \times 10^{-3})$ from the integral breadth analysis, neglecting the presence of any growth faults. The growth fault probability, β, from the present analysis is very small ($\sim 2.07 \times 10^{-3}$), being within the range of experimental error and thus appears to be negligible in the cold-worked state, in conformity with the earlier observations [2, 4-5] with plastically deformed hcp metals and alloys. Thus, considering β to be zero, the values of the deformation fault probability, α, for the respective planes, have also been calculated and the mean value of $\alpha(\simeq 9.38 \times 10^{-3})$ has been obtained for titanium (Table II). For the partially recovered state of titanium, both the deformation and growth faults seem to anneal out with negligible concentrations of these ($\alpha \sim 0.06 \times 10^{-3}$ and $\beta \sim 2.05 \times 10^{-3}$) lying within experimental limitations (Table II). Considering any absence of growth faults, the

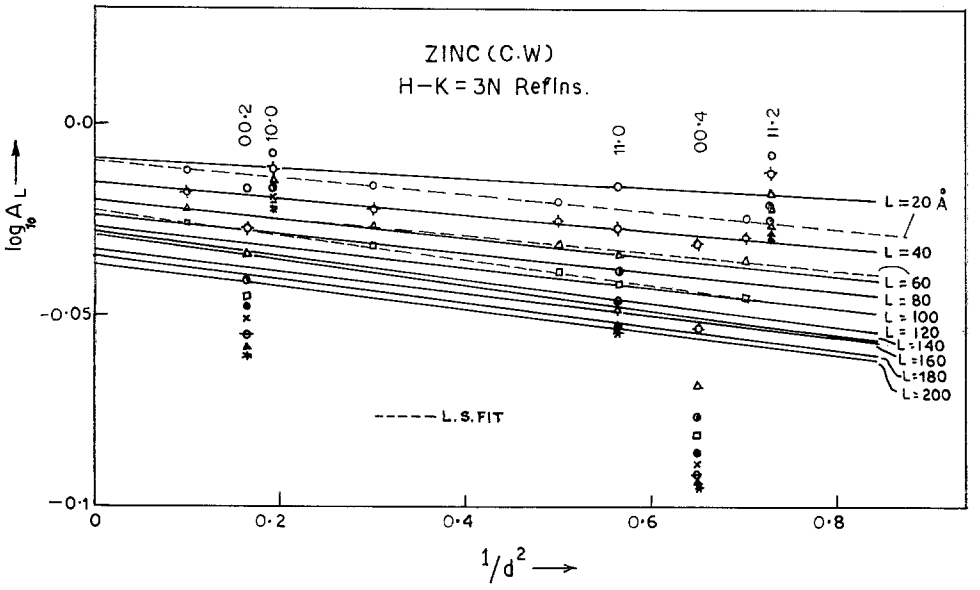

Figure 8 The plot of $\log_{10} A_L$ versus $1/d^2$ for values of L for cold-worked zinc.

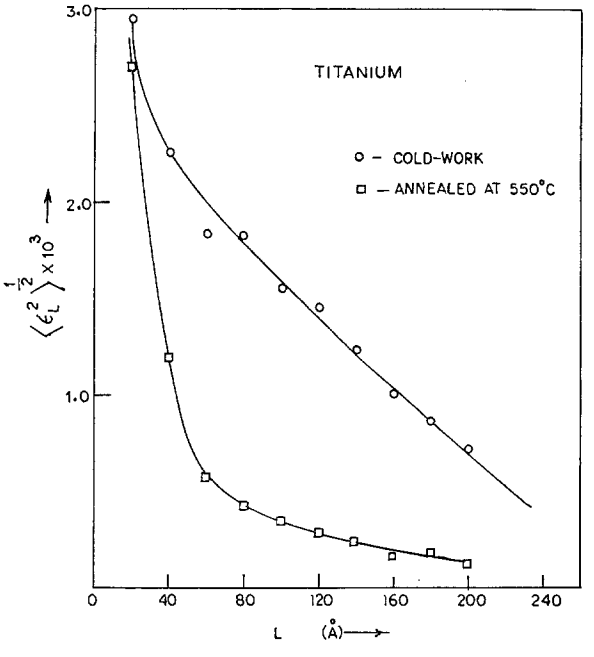

Figure 9 The plot of r.m.s. strain $\langle \epsilon_L^2 \rangle^{\frac{1}{2}}$ versus L for cold-worked titanium.

mean value of α for this recovered state is $\sim 1.81 \times 10^{-3}$, which may be considered to be negligible.

For magnesium, the deformation and growth fault probabilities, α and β, are found to be much less than those obtained for zirconium and titanium and are of the order of 0.63×10^{-3} and 0.21×10^{-3}, respectively (Table II). These values lie well within the range of experimental error and the value of α is slightly less than 1.1×10^{-3} as reported earlier by Lele and Anantharaman [4]. This result indicates that the probability of the incidence of both deformation and growth faults in this material seems to be

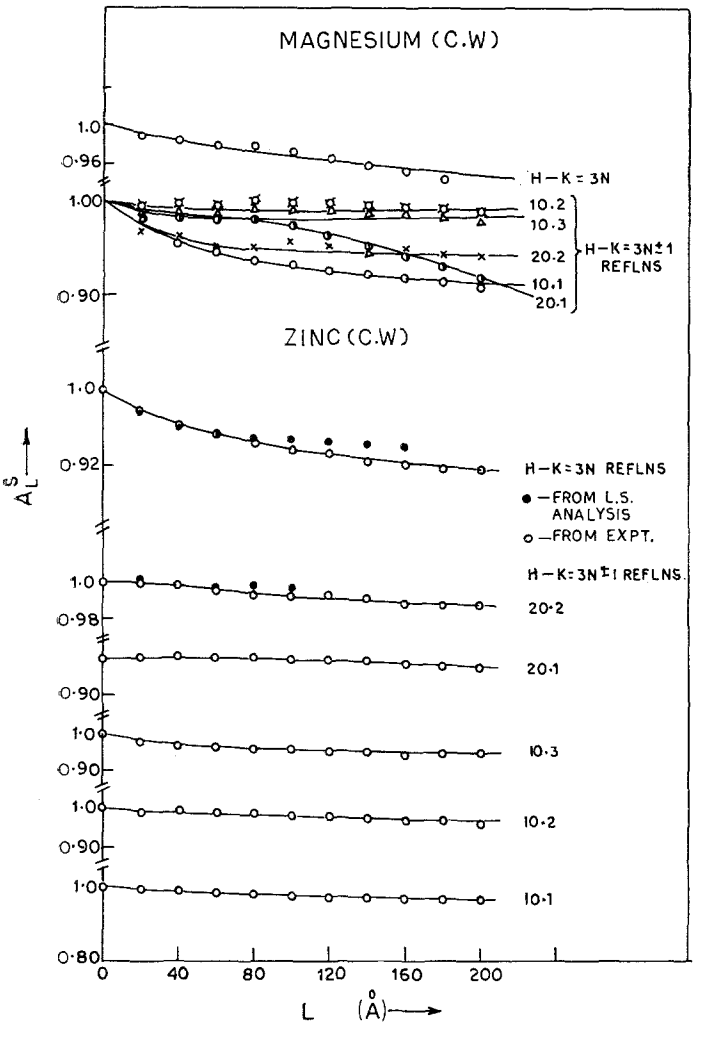

Figure 10 The plot of distortion corrected size coefficients A_L^S versus L, for cold-worked magnesium and zinc.

negligible. If growth faults are considered to be absent, the α values may also be calculated for each individual fault-affected reflection (Table II). The very small value for each reflection, except for the 10.1 and 20.2 reflections where it is slightly higher ($\sim$ 1.93 $\times$ 10^{-3}), indicates that the entire observed broadening is due to a strain, isotropic in nature, as the domain size is very large. This has also been observed from the close proximity of the points in the log plots of A_L with $1/d^2$ for all ten recorded reflections of magnesium. The average domain size obtained from this plot is $\sim$ 2000 Å and the r.m.s. strain is $\sim$ 0.61 $\times$ 10^{-3} (Table III); these values are very close to 1650 Å and 0.71 $\times$ 10^{-3}, obtained from the consideration of fault-unaffected reflections (Table I). However, they differ very little as they are very close to the experimental and analytical limits of determination. In the case of zinc too, similar observations on the presence of deformation and growth faults could be made from the closeness between values of the effective domain sizes, D_e (Å), for the fault-affected reflections, and average domain size, D (Å), for the fault-unaffected reflections (Tables I and II). The close proximity of points in the log plots has also been observed here for all reflections. The values of the average domain size and r.m.s. strains from this plot are $\sim$ 1120 Å and $\sim$ 0.44 $\times$ 10^{-3}, respectively (Table III), which are very close to the respective ones ($\sim$ 1060 Å and $\sim$ 0.57 $\times$ 10^{-3}, Table I) obtained from the fault-unaffected reflections only. These observations are, there-

TABLE III Average domain size D and strain $\langle \epsilon_L^2 \rangle^{\frac{1}{2}}$ for magnesium and zinc considering all observed reflections

Magnesium			Zinc		
Reflections according to θ	D (Å)	$\langle \epsilon_L^2 = 100\ \text{Å} \rangle^{\frac{1}{2}} \times 10^3$	Reflections according to θ	D (Å)	$\langle \epsilon_L^2 = 100\ \text{Å} \rangle^{\frac{1}{2}} \times 10^3$
10.0			00.2		
00.2			10.0		
10.1			10.1		
10.2	2000	0.61	10.2	1120	0.44
11.0			10.3		
10.3			11.0		
11.2			00.4		
20.1			11.2		
00.4			20.1		
20.2			20.2		

fore more or less identical to those of magnesium.

The dislocation density, ρ, calculated from the Equations 4 to 6 using the values of average domain size, D, and the Gaussian distribution of r.m.s. strains, ϵ_L, at an average column length $L = 100$ Å, are shown in Table I for titanium, magnesium and zinc. In the cases of magnesium and zinc, these values have been found to be less by one order of magnitude than that of titanium in the cold-worked state. This is quite evident from the relatively high values of domain size, D, in both magnesium and zinc (Table I).

The magnitude of the stacking fault energy, γ, which bears an inverse relationship to the stacking fault probability, α, has been estimated for titanium and magnesium from Equation 11 using the values of α and β given in Tables I and II and of shear modulus, μ from [14]. The values of γ are shown in Table IV where values of α are considered to be high for all the fault-affected and also for less-affected planes. In these cases, a very low stacking fault probability, α (Table II) implies a high stacking fault energy for the basal planes of these materials. This is in agreement with the theoretical considerations of Seeger [15] from the electronic structure of the hexagonal materials. However, this differs considerably from the appreciably low values obtained here for the stacking fault energy, γ (Table IV), for basal slip and also the existing experimental observations. Recent electron microscopic observations with single crystals of zirconium [16, 17] have shown a small value for the stacking fault energy on the prism planes and predicted that in zirconium and titanium, both having a similar c/a ratio, the prismatic slip is more favourable to basal slip. In a very recent study [18] on cold-rolled titanium sheet, it has been observed that the active primary slip system is of the prismatic $\{1\bar{1}00\}\langle 11\bar{2}0\rangle$ type, while the secondary system is either the prismatic or pyramidal type. It has, however, been suggested that in certain orientations of load directions, the basal slip mode rarely observed in this study may be the primary slip system. In the case of magnesium, Seeger [19] has reported a value of 60 erg cm^{-2} for γ from the flow stress analysis. Price [20] and Harris and Masters [21] have, however, from electron microscopy indicated a very high stacking fault energy for basal slip in magnesium. For zinc, Bocek and Kaska [22] have obtained a value of 370 erg cm^{-2} for γ, and

TABLE IV Stacking fault energy, γ for hexagonal titanium and magnesium

Sample	L.S. value of α from reflections	γ (erg cm^{-2})	Mean value of α from reflections	γ (erg cm^{-2})
Ti	10.1	3.2	10.1	12.2
	10.2		10.3	
	10.3		10.2	
Mg	20.1	2.1	20.1	24.7
	20.2		10.3	
			10.2	

Price [20], based on the results of Berghezan *et al.* [23] from transmission electron microscopy, showed the value to be quite low and in the order of 30 erg cm^{-2}.

From the above observations it appears, therefore, that a wide diversity in the values of the stacking fault energy determined from various existing methods of analyses exists. This is also understandable from the critical analysis of Gallagher and Liu [24] on the stacking fault energy measurements by several methods. In our present analysis, the determination of γ is not only influenced by the magnitude of α, but also from the estimates of the dislocation density, ρ, based on certain dislocation networks which may develop in the cold-worked material. This, it is difficult to predict the easiest slip mode in these materials, in terms of either the basal or prismatic mode, from the consideration of the magnitudes of stacking fault energy. However, very small concentrations of stacking faults, as observed in the present X-ray line shape analysis for titanium as well as for zirconium in Part 1, suggest that basal slip may not be a favourable slip mode and may be inhibited by prismatic slip [16, 17]. In the case of magnesium and zinc, where the basal slip of the form $(0001)\langle 11\bar{2}0\rangle$ has been observed to be a favourable slip mode [16, 25], negligible concentrations of stacking faults may also be associated with the recovery effects as observed from the large domain sizes (Table I). Since the X-ray diffraction effects in the case of slip modes, other than the basal slip, are yet to be understood, it is, therefore, necessary to perform detailed electron microscopic observations of these hexagonal materials to elucidate which is the easiest slip mode.

4. Conclusions

From the detailed Fourier analysis of the maximum number of observable X-ray diffraction profiles from the cold-worked magnesium, zinc, titanium and partially recovered state of titanium, the following conclusions may be tentatively drawn:

(1) The results of line-shape analysis for titanium are found to be consistent with those observed in Part 1 for zirconium;

(2) The existence of a small anisotropy in both domain sizes and strains has been observed from the log plots of fault-unaffected, as well as fault-affected, reflections in the cases of magnesium and zinc. This indicates that these effects remain more or less uniform for all the observed reflections and that the effects due to the stacking faults are quite insignificant for magnesium and zinc. The average domain size values for magnesium and zinc are quite high compared to those for titanium and also zirconium (Part 1), indicating considerable room-temperature recovery in the domain size broadening effect. A small recovery has been observed for titanium on annealing;

(3) The least-squares analysis of fault-affected reflections has yielded very small concentrations of deformation and growth stacking faults in titanium, and negligible concentrations in magnesium in the cold-worked states. The presence of these could not be detected in zinc;

(4) The stacking fault energy in titanium and magnesium has been estimated from the results obtained, and found to be quite low. However, it appears to be difficult to obtain a clear picture of the primary slip mode (either basal or prismatic) on the basis of stacking fault energy measurments in these materials.

Acknowledgements

The authors are grateful to Professor A. K. Barua for his active interest in the work. One of us (S.K.C.) is also grateful to the Council of Scientific and Industrial Research (New Delhi) for financial assistance.

References

1. B. E. WARREN, "X-ray Diffraction" (Addison-Wesley, Reading, Mass. (1969).
2. S. K. CHATTERJEE and S. P. SEN GUPTA, *J. Mater. Sci.* **9** (1974) 953.
3. J. SPREADBOROUGH and J. W. CHRISTIAN, *Proc. Phys. Soc. (London)* **74** (1959) 609.
4. S. LELE and T. R. ANANTHARAMAN, *Z. Metallk.* **58** (1967) 37.
5. R. K. GUPTA, P. RAMA RAO and T. R. ANANTHARAMAN, *Z. Metallk.* **63** (1972) 575.
6. S. LELE and T. R. ANANTHARAMAN, *Phys. Stat. Sol.* **5** (1964) K 121.
7. G. B. MITRA and N. K. MISRA, *Acta Cryst.* **22** (1967) 454.
8. A. R. STOKES, *Proc. Phys. Soc. (London)* **61** (1948) 382.
9. G. K. WILLIAMSON and R. E. SMALLMAN, *Phil. Mag.* **1** (1956) 34.
10. R. E. SMALLMAN and K. H. WESTMACOTT, *Phil. Mag.* **17** (1957) 669.
11. L. F. VASSAMILLET, *J. Appl. Phys.* **32** (1961) 778.
12. D. HULL, "Introduction to dislocations" (Pergamon Press, London, 1968) Ch. 5 and 6.
13. A. H. COTTRELL, "Dislocation and plastic flow in crystals" (Clarendon Press, Oxford, 1933) p. 74.

14. G. SIMMONS and H. WANG, "Single crystal elastic constants and calculated aggregate properties" (M.I.T. Press, Cambridge, 1971) pp. 319, 326.
15. A. SEEGER, "Dislocation and Mechanical Properties of Crystals" (Wiley, New York, 1957) p. 243.
16. A. AKHTAR and E. TEGHTSOONIAN, *Acta Met.* **19** (1971) 655.
17. A. AKHTAR, *Acta Met.* **21** (1973) 1.
18. D. STRECHTMAN and D. G. BRONDON, *J. Mater. Sci.* **8** (1973) 1233.
19. A. SEEGER, S. MADER and H. KRONMULLER, "Electron microscopy and strength of crystals", edited by G. Thomas and J. Washburn (Interscience, New York, 1963) p. 665.
20. P. B. PRICE, *ibid* p. 41.
21. J. E. HARRIS and B. C. MASTERS, *Phys. Stat. Sol.* **9** (1965) K 181.
22. M. BOCEK and V. KASKA, *Phys. Stat. Sol.* **4** (1964) 325.
23. A. BERGHEZAN, A. FOURDEUX and S. AMELINCKX, *Acta Met.* **9** (1961) 464.
24. P. C. J. GALLAGHER and Y. C. LIU, *Acta Met.* **17** (1969) 127.
25. W. TYSON, *ibid* **15** (1967) 574.

Received 28 August 1974 and accepted 7 January 1975